

Full Length Research Paper

Kinetic studies of adsorption of palmitate and laurate soaps onto some metal ores in aqueous media

Millicent U. Ibezim-Ezeani* and Alphonso C. I. Anusiem

Department of Pure and Industrial Chemistry, University of Port Harcourt, P. M. B. 5323, Choba, Port Harcourt, Nigeria.

Accepted 19 November, 2009

The kinetics of adsorption of sodium-palmitate and sodium-laurate onto galena, hematite and cassiterite in aqueous media was investigated at various concentrations, times and temperatures. Experimental results were analysed using the pseudo-first and pseudo-second order kinetic models. The pseudo-first order model with higher correlation coefficient values described the adsorption kinetics better than the pseudo-second order model. The rate constant from the pseudo-first order model [0.109 min^{-1} for galena, 0.102 min^{-1} for hematite, 0.085 min^{-1} for cassiterite (in the sodium-palmitate adsorption) and 0.127 min^{-1} for galena, 0.109 min^{-1} for hematite, 0.095 min^{-1} for cassiterite (in the sodium-laurate adsorption) at 29°C] show these rates in the order: galena > hematite > cassiterite for the adsorbents; and sodium-laurate > sodium-palmitate for the adsorbates. Some kinetic parameters were computed and the values obtained indicate that the adsorption processes occurred at reasonable rate, low temperature and low energy suggesting physical adsorption as the dominant process.

Key words: Kinetics, adsorption, soap, collector reagent, pseudo-first order.

INTRODUCTION

Soap molecules exhibit amphipatic characteristics and as such are able to alter the surface properties of a system by their preferential orientation for optimum interaction at the interface. The rates and mechanisms involved in the preferential adsorption of molecules of sodium-palmitate and sodium-laurate soaps (adsorbates) on the surfaces of adsorbents (galena, hematite and cassiterite) in aqueous phase were examined in this investigation. These rates and mechanisms are governed by adsorption conditions, nature of the adsorbate and adsorbent (Ho and McKay, 1998a; Abia et al., 2006). A good knowledge of the adsorption kinetics is of paramount importance in designing, running and improving the efficiency of industrial adsorption plants and processes. Numerous applications of adsorption kinetic equations have been reported: Krishnan and Anirudhan (2003) used adsorption kinetic equations in the kinetics and equilibrium processes for the removal of Cd (II) from aqueous solutions by steam-activated sulphurised car-

bon prepared from sugar-cane baggase pith and found the process of adsorption to follow pseudo-second order kinetics. The increase in rate of adsorption with increasing temperature was described by the Arrhenius equation and they obtained an activation energy of 18.28 kJ/mol indicating a chemical adsorption process with weak interactions between the adsorbent and adsorbate (Ho et al., 2001). Similar findings were reported by Ho (2006), Horsfall et al. (2006), Kim et al. (2005), Ofomaja et al. (2005), Preetha and Viruthagiri (2005), Cordero et al. (2004), Demirbas et al. (2004), Baeza et al. (2003) and Quek et al. (1998) in their various study. Sorption studies of Ag (I), Cd (II) and Pb (II) ions on sulphhydryl hemp fibers by Tofan and Paduraru (2004) confirmed the applicability of the Lagergren pseudo-first order rate equation. Ofor and Anusiem (1999) determined the rate of adsorption of oleate soap onto a Nigerian hematite in an aqueous medium from 29 to 60°C using the differential analysis method. The activation energy and frequency factor were determined to be $57.1 \text{ kJmol}^{-1}\text{K}^{-1}$ and $4.0 \times 10^3 \text{ litermol}^{-1}\text{min}^{-1}$ respectively, indicating that the chemical processes are the slow, rate-determining step and that the reaction proceeds relatively fast. Also, their results showed that the adsorption process was first-order

*Corresponding author. E-mail: millibejmj@yahoo.com. Tel: +2347039450740.

kinetics with respect to oleate concentration in the bulk solution and that the rate constant increased with an increase in reaction temperature. In this study, the kinetic behaviour of the adsorption of sodium-palmitate and sodium-laurate onto galena, hematite and cassiterite in aqueous solutions is determined and may be used for the optimal design of an appropriate mineral flotation processing plant with sodium-palmitate and sodium-laurate as collector reagents.

MATERIALS AND METHODS

Galena assaying 59.3% lead (obtained from Enyigba-Abakaliki, Nigeria), hematite assaying 76.9% iron (obtained from Itakpe, Nigeria) and cassiterite assaying 58.7% tin (obtained from Jos, Nigeria) are the metal ores used for this study. The samples were crushed in the laboratory jaw and roll crushers. Gravimetric method of jigging and tabling was employed in removing siliceous materials, while magnetic separation method was used in separating magnetic materials from the ore sample. Sieve analyses were performed using the British standard sieve plates to obtain samples of galena – 65 micron, hematite – 70 micron and cassiterite – 65 micron. Mineralogical analysis of the ore samples was performed with volumetric and spectrophotometric (Buck scientific atomic absorption spectrophotometer - model 205A) methods of analyses. Solutions of reagents were prepared with distilled deionised water, sodium hydroxide and hydrochloric acid solutions were used for pH adjustments. BDH chemical reagents analar grade (of not less than 98% purity) were used in this study. Determination of specific surface area (SSA) was done by the ethylene-glycol-monethyl ether (EGME) method (Cerator and Lutenegger, 2002). Soap preparation was performed by saponification reaction (Tooley, 1976).

DETERMINATION OF KINETIC PARAMETERS

0.5 g of sample (galena / hematite / cassiterite) was added to 40 cm³ of 0.001 mol/L soap solution in a flask, corked and shaken in a mechanical shaker (120 oscillations per min.) for one hour at 29°C. The mixture was centrifuged, decanted and filtered until a clear filtrate was obtained. The soap concentration was obtained from the calibration graph as earlier described. The adsorption capacity (q_e) in mol/g, was determined. This experiment was repeated at different temperatures of 40, 50 and 60°C. In another set of experiments, 0.5 g of the sample (galena / hematite / cassiterite) was placed in several flasks containing 40 cm³ of 0.001 M sodium-palmitate / sodium-laurate solution at 29°C. The flasks were shaken vigorously and samples withdrawn at different time intervals, centrifuged and filtered until a clear filtrate was obtained. The conductance of the clear filtrate was measured and the amount of adsorbate adsorbed obtained from the calibration graph. The adsorption capacity (q_t) in mol/g was determined at different time intervals. The experiment was repeated at temperatures of 40, 50 and 60°C.

DATA EVALUATION

The concentration of soap samples were obtained from the calibration plots of the metal soaps based on Kohlrausch law equation in Equation 1 (Atkins, 1998).

$$\Lambda_m = \Lambda_m^o - KC \quad (1)$$

Where; Λ_m is the molar conductivity, Λ_m^o is the limiting molar conductivity, C is the concentration of the solution and K is a constant. The adsorption capacity (q_e) in mol/g was determined using the mass balance equation (Horsfall et al., 2006; Zulkali et al., 2006).

$$q_e = \frac{V}{m} (C_o - C_e) \quad (2)$$

The adsorption capacity (q_t) at time, t in mol/g was determined using Equation 3 (Demirbas et al., 2004).

$$q_t = \frac{V}{m} (C_o - C_t) \quad (3)$$

Where; C_e is the soap concentration in solution (mol/L) at equilibrium, C_t is the soap concentration in solution (mol/L) at time, t, C_o is the initial soap concentration in solution, V is volume of initial soap solution used (L) and m is mass of adsorbent used (g). Some kinetic models used in describing adsorption rates and mechanisms are presented in equations 4 and 5.

The pseudo-first-order equation of Lagergren (Ho, 2004; Ho and Mckay, 1998a) is expressed as:

$$\log (q_e - q_t) = \log (q_e) - \frac{k}{2.303} t \quad (4)$$

Where; q_e and q_t are the adsorption capacity at equilibrium and at time, t respectively (mol/g) and k is the rate constant of pseudo-first-order adsorption (min⁻¹). A plot of $\log (q_e - q_t)$ against t is linear and k can be determined from the slope.

The pseudo-second-order chemisorption kinetic rate equation (Ho and Mckay, 1998a, b; Ho, 2004) is expressed as:

$$\frac{t}{q_t} = \frac{1}{k_2 q_e^2} + \frac{1}{q_e} t \quad (5)$$

k_2 represents the pseudo-second-order rate constant. A plot of t/q_t as a function of t is linear and the value of k_2 is determined from the slope and intercept.

An assessment of the rate of adsorption with temperature is described by Arrhenius equation (Krishnan and Anirudhan, 2003; Manilla et al., 2001; Anusiem, 2000; Atkins, 1998) as in Equation 6.

$$\ln k = \ln A_o - \frac{E_{ads}}{RT} \quad (6)$$

Where; k is the rate constant, A_o is the frequency factor, E_{ads} is activation energy of adsorption, R is the gas constant, T is temperature.

The coefficient of determination (R^2) measurements were used to determine the best fitting kinetic model (Chase and Brown, 1992).

RESULTS AND DISCUSSION

SPECIFIC SURFACE AREA OF ADSORBENTS

Calculations from experimental results and sample ana-

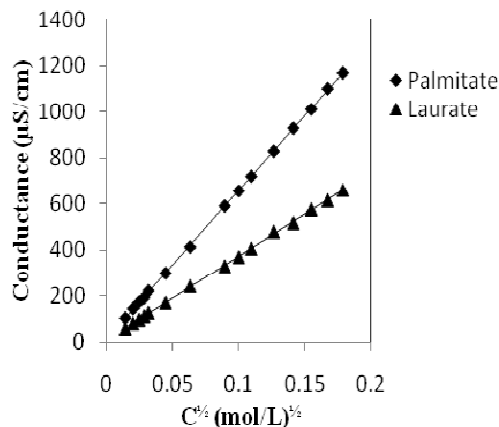


Figure 1. Plot of conductance versus soap concentration.

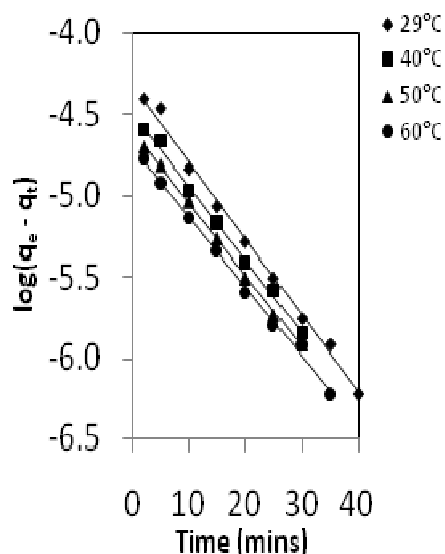


Figure 2. Plot of pseudo-first order kinetics for adsorption of sodium-palmitate onto Galena.

lysis show that the specific surface area of galena is $128.7 \text{ m}^2/\text{g}$, hematite is $118.5 \text{ m}^2/\text{g}$ and cassiterite is $88.1 \text{ m}^2/\text{g}$. These values indicate that the surface area is in the order: galena > hematite > cassiterite. It is expected that if the specific surface area is the primary factor for adsorption, that the adsorption capacity will be greatest for galena. Ho (2006), Horsfall et al. (2004), Horsfall and Abia (2003) reported increased adsorption capacity with increasing surface area in their various studies.

CALIBRATION OF CONDUCTOMETER

Plots of the conductance of sodium-palmitate / sodium-laurate against the square root of initial soap concentrations are linear (Figure 1). This was used for subsequent

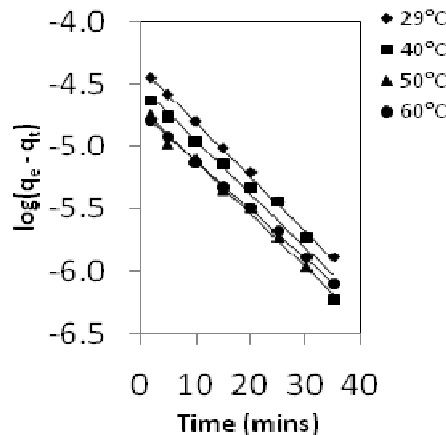


Figure 3. Plot of pseudo-first order kinetics for adsorption of sodium-palmitate onto hematite.

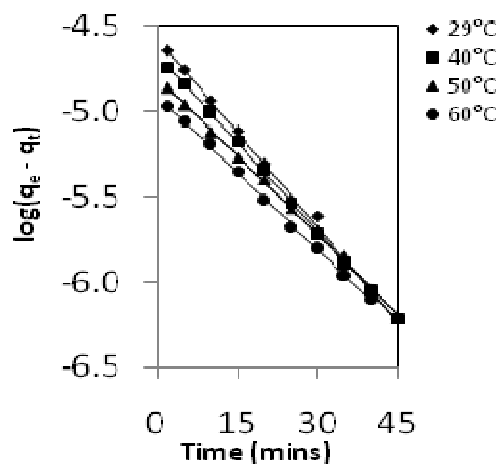


Figure 4. Plot of pseudo-first order kinetics for adsorption of sodium-palmitate onto cassiterite.

determination of concentration of the soaps in the various experiments.

KINETICS STUDIES

The pseudo-first order Lagergren kinetic and the pseudo-second order kinetic models were used to fit the experimental data. The best fits in the whole data range were found with the pseudo-first order model since the coefficient of determination were higher for the pseudo-first order rate equation as represented in Tables 1 and 2. The pseudo-first order Lagergren kinetic model was therefore used to analyze our experimental data at various temperatures and time and presented in Figures 2 to 4 for the sodium-palmitate and Figures 5 to 7 for sodium-laurate adsorption.

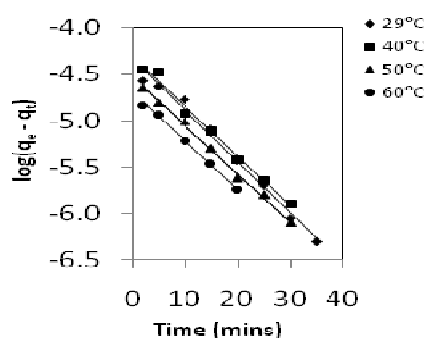
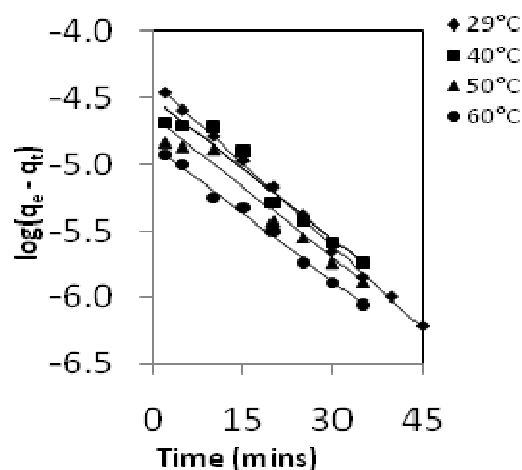
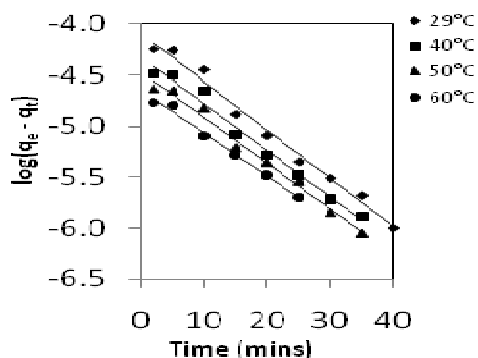
The values of the rate constants from the kinetic models

Table 1. Comparison of Coefficients of Determination for the Sodium-Palmitate Adsorption.

Temp °C	Galena		Hematite		Cassiterite	
	First-Order	Second-Order	First-Order	Second-Order	First-Order	Second-Order
29	0.9952	0.6809	0.9984	0.9699	0.9972	0.9922
40	0.9963	0.9345	0.9618	0.9983	0.9995	0.9975
50	0.9988	0.9959	0.9936	0.9939	0.9983	0.9994
60	0.9959	0.9960	0.9992	0.9929	0.9991	0.9812

Table 2. Comparison of coefficients of determination for the Sodium-Laurate Adsorption.

Temp. °C	Galena		Hematite		Cassiterite	
	First-Order	Second-Order	First-Order	Second-Order	First-Order	Second-Order
29	0.9870	0.2452	0.9874	0.4093	0.9982	0.9884
40	0.9888	0.0071	0.9838	0.0078	0.9537	0.0154
50	0.9967	0.9972	0.9877	0.7975	0.9292	0.1128
60	0.9969	0.9838	0.9896	0.7319	0.9936	0.9531

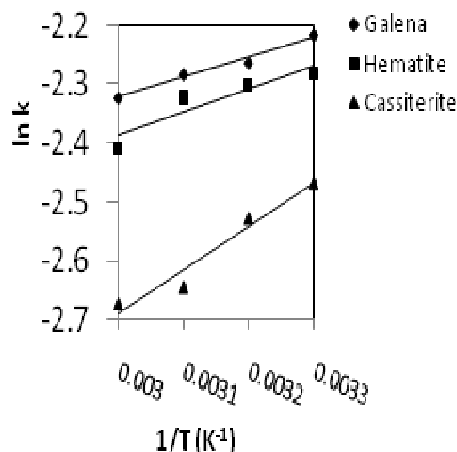
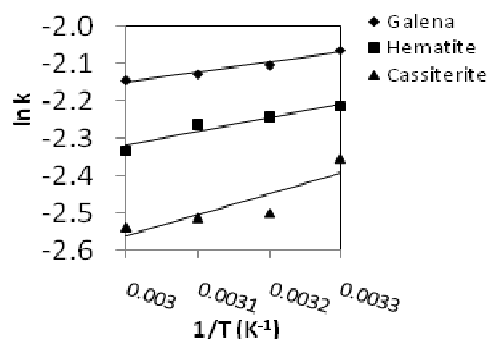
**Figure 5.** Plot of pseudo- first order kinetics for adsorption of sodium-laurate onto galena.**Figure 7.** Plot of pseudo- first order kinetics for adsorption of sodium-laurate onto cassiterite.**Figure 6.** Plot of pseudo- first order kinetics for adsorption of Sodium-Laurate onto hematite.

for the sodium-palmitate and sodium-laurate adsorption at different temperatures are presented in Table 3.

Our results show that there is a decrease in rate constant with increase in temperature from 29 to 60°C. It is possible that the structure of the adsorbate molecules are distorted as their melting points (70°C for sodium-palmitate and 66°C for sodium-laurate) are approached, thereby affecting their proper orientation and interaction at the adsorption site, hence the decreased uptake of the adsorbate ions leading to the decrease in rate constant. The values of the rate constant are in the order: galena > hematite > cassiterite. This could be due to the larger surface area of galena compared to that of hematite and cassiterite as earlier discussed. Results obtained also show that the sodium-laurate had a higher adsorption capacity than sodium-palmitate. It could be that the smaller carbon-chain of the laurate (12 carbon atoms) soap enhanced better migration and interaction of the

Table 3. Rate constant (k) at different temperatures.

Temp. (°C)	Sodium-Palmitate			Sodium-Laurate		
	Galena k (min ⁻¹)	Hematite k (min ⁻¹)	Cassiterite k (min ⁻¹)	Galena k (min ⁻¹)	Hematite k (min ⁻¹)	Cassiterite k (min ⁻¹)
29	0.109	0.102	0.085	0.127	0.109	0.095
40	0.104	0.100	0.080	0.122	0.106	0.082
50	0.102	0.098	0.071	0.119	0.104	0.081
60	0.098	0.090	0.069	0.117	0.097	0.079

**Figure 8.** Plot of natural logarithm of rate constant at different temperatures for sodium-palmitate adsorption.**Figure 9.** Plot of natural logarithm of rate constant at different temperatures for sodium-laurate adsorption.

adsorbate to the active adsorbent sites than the longer carbon-chain of palmitate (16 carbon atoms) soap.

The plots of $\ln k$ versus $1/T$ are linear (Figure 8 for sodium-palmitate and Figure 9 for sodium-laurate) as described by Arrhenius equation (Equation 6).

The values of E_{ads} (activation energy of adsorption) were computed from the slope of the plots and presented in Table 4.

The negative values of E_{ads} indicate that the lower tem-

Table 4. E_{ads} for sodium-palmitate and sodium-laurate

Adsorbent	E_{ads} (kJ/mol)
Galena (sodium-palmitate)	-2.81
Hematite (sodium-palmitate)	-3.29
Cassiterite (sodium-palmitate)	-6.19
Galena (sodium-laurate)	-2.25
Hematite (sodium-laurate)	-3.07
Cassiterite (sodium-laurate)	-4.70

peratures favour the adsorption of both adsorbates onto the adsorbents. The values of the E_{ads} for the adsorbents are in the order: galena > hematite > cassiterite. The higher values of E_{ads} for galena compared to that for hematite and cassiterite indicate that more energy is required to form the activated complex in the case of galena which has larger surface area than hematite and cassiterite. Also our results show that the values of the E_{ads} for sodium-palmitate are lower than that of sodium-laurate for the different adsorbents suggesting that the sodium-palmitate adsorption has a lower potential energy barrier than sodium-laurate apparently due to their structural difference as previously discussed.

Conclusion

The study focused on the application of the pseudo-first order and pseudo-second order kinetic models for predicting the rates and mechanisms involved in the adsorption of sodium-palmitate and sodium-laurate onto galena, hematite and cassiterite in aqueous solutions. Kinetically, the adsorption processes were described by the Lagergren pseudo-first order model and was found to occur in about 45 min at reasonable rate and with low activation energy. The level of adsorption of both adsorbate on the surfaces suggests that both the laurate and palmitate show a reasonable degree of surface coverage at low temperature and energy that may warrant their use as collector reagents in metal ore processing through the froth flotation technique.

REFERENCES

- Abia AA, Didi OB, Asuquo ED (2006). Modeling of Cd^{2+} Sorption Kinetics from Aqueous Solutions onto Some Thiolated Agricultural Waste Adsorbents. *J. Appl. Sci.* 6(12): 2549-2556.
- Anusiem ACI (2000). Principles of General Chemistry – A programmed Approach. Revised edn. Versatile publishers, Umuahia – Abia State, Nigeria.
- Atkins PW (1998). Physical Chemistry, 6th edn, Oxford University Press, New York pp.775-777.
- Baeza H, Guzman M, Ortega P, Vera L (2003). Corrosion Inhibition of Copper in 0.5M Hydrochloric Acid by Thiadiazole-2,5-dithiol. *J. Chilean Chem. Soc.* 48(3): 33-40.
- Cerato AB, Lutenegeger AJ (2002). Determination of Surface area of fine-grained soils by the Ethylene glycol Monoethyl ether (EGME) Method. *Geotech. Testing J.* 25(3): 1-7.
- Cordero B, Lodeiro P, Herrero R, Sastre de Vicente ME (2004). Biosorption of Cadmium by *Fucus Spiralis*, *Environ. Chem.* 1: 180-187.
- Demirbas E, Mehmet K, Elif S, Tuncay O (2004). Adsorption Kinetics for the Removal of Chromium (vi) from Aqueous Solutions on the Activated Carbons Prepared from Agricultural Wastes. *Water SA.* 3(4): 533-539.
- Ho YS (2004). Comments on an Evaluation of Copper Biosorption by a Brown Seaweed Under Optimized Condition by Aritunes WM, Luna AS, Henriques CA, Da costa ACA. *J. Electronic Biotechnol.* 7(3): 228-237.
- Ho YS (2006). Second-order Kinetic Model for the Sorption of Cadmium onto Tree fern: A Comparison of Linear and non-Linear Methods. *Water Res.* 40: 119-125.
- Ho YS, McKay G (1998a). A Two-Stage Batch Sorption Optimized Designed for Due Removal to Minimize Contact Time. *Trans. Chem E.* 76b: 313-138.
- Ho YS, McKay G (1998b). A comparison of Chemisorption Kinetic, Models Applied to Pollutant Removal On various Sorbents. *Institution of Chemical Engineers Trans. Chem E.* 76b: 332-340.
- Ho YS, Ng JCP, McKay G (2001). Removal of Lead (II) from Effluents by Sorption of Peat Using Second-order Kinetics. *Sep. Sci. Technol.* 36: 241-261.
- Horsfall M Jr., Abia AA (2003). Sorption of Cadmium (II) and Zinc (II) ions from Aqueous Solutions by Cassava Waste Biomass (*Manihot esculenta* Vanz). *Water Res.* 37: 4913-4923.
- Horsfall M Jr., Abia AA, Spiff AI (2006). Kinetic Studies on the Adsorption of Cd^{2+} , Cu^{2+} and Zn^{2+} ions from Aqueous Solutions by Cassava (*Manihot esculenta* Vanz) Tuber Bark Waste. *Bioresour. Tech* 97: 283-291.
- Horsfall M Jr., Spiff AI, Abia AA (2004). Studies on the Influence of Mercaptoacetic Acid (MAA) Modification of Cassava (*Manihot esculenta* Cranz). Waste biomass on the Adsorption of Cu^{2+} and Cd^{2+} from Aqueous solution. *Bull. Korean Chem. Soc.* 5(7): 969-976.
- Kim TY, Sun-Kuu P, Sung-ony C, Kim HB, Kang Y, Kim SD, Kim SJ (2005). Adsorption of Heavy Metals by Brewery Biomass. *Korean J. chem. Eng.* 22(1): 91-98.
- Krishnan KA, Anirudhan TS (2003). Removal of Cadmium (II) from Aqueous Solutions by Steam-activated Sulphurised Carbon prepared from Sugar-Cane Baggase Pith: Kinetics and Equilibrium Studies. *Water SA.* 29(2): 147-156.
- Manilla PN, Ogali RE, Uzoukwu BA (2001). Undergraduate Chemistry: Fundamental Principles. Timi Hyacinth Publishers, Lagos, Nigeria. pp. 687-688.
- Ofomaja AE, Unuabonah EI, Abiola ON (2005). Removal of Lead from Aqueous Solution by Palm Kernel Fibre. *S. Afr. J. Chem.* 58: 127-130.
- Ofor O, Anusiem ACI (1999). Kinetics of Oleate Adsorption at a Nigerian Hematite-Water Interface. *J. Colloid Interface Sci.* 220: 219-223.
- Preetha B, Viruthagiri T (2005). Biosorption of Zinc (II) by *Rhizopus arrhizus*: Equilibrium and Kinetic Modelling. *Afr. J. Biotechnol.* 4(6): 506-508.
- Quek SY, Wase DAJ, Forster CF (1998). The Use of Sago Waste for the Sorption of Lead and Copper. *Water SA.* 24(3): 251-256.
- Tofan L, Paduraru C (2004). Sorption Studies of Ag (I), Cu (II) and Pb (II) Ions Sulphydryl Hemp Fibers. *Croatia Chem. Acta CCACAA* 77(4): 581-586.
- Tooley P (1976). Experiments in Applied chemistry, Published by John Murray, London 29p.
- Zulkali MMD, Ahmad AL, Norulakmal NH (2006). Ovyza Sativa L. Husk as Heavy Metal Adsorbent Optimization with Head as Model Solution. *Bioresour. Technol.* 97: 21-25.